PV-STATCOM in Photovoltaic Systems under Variable Solar Radiation and Variable Unbalanced Nonlinear Loads

Youssef Ait El Kadi, Fatima Zahra Baghli, and Yassine Lakhal
Laboratory of Engineering and Applied Technologies, Higher School of Technology, Sultan Moulay Slimane University, Beni Mellal, Morocco
Email: youssefaitelkadiusms@gmail.com

***Abstract*—The paper focuses on an efficient method to compensate the harmonics and zero-sequence component caused by the variable unbalanced nonlinear loads. The studied compensator is based on the conventional Static Compensator (STATCOM) which is supplied by a photovoltaic generator rather than the storage passive components. That constitutes a Photovoltaic Static Compensator (PV-STATCOM). In addition to the active power production, this PV-STATCOM will improve the quality of the electric grid highly disturbed without any additional devices and costs. The used control strategy is based on the instantaneous power method and current control. The obtained results show the benefits of the photovoltaic active filter compensator to improve the energy quality. Specially, the Total Harmonic Distortion (THD) is decreased from 28.80 % to 2.03 %. The zero-sequence component of the load currents is reduced from 31.50 % to 4.26 %. The results prove also a high stabilization and limitation of the harmful repercussions of the compensator on the photovoltaic station and an automatic adapting to the solar variable radiation and to the unbalanced nonlinear load variations.**

***Index Terms*—Harmonic, instantaneous power, PV-STATCOM, unbalanced nonlinear load, variable load**

I. Introduction

In recent decades, the use of power electronics equipment and other nonlinear loads in industry has contributed to the decrease of the quality of energy in the distribution grid. Indeed, the static converters (rectifiers, dimmers, frequency-converters) have proliferated in the industrial devices and domestic equipments. Certainly, the use of these converters in electrical energy conversion has significantly contributed to improve the performance and efficiency of these systems. However, these converters decrease the quality of the current and the voltage of the distribution grid. Despite the sinusoidal supply voltages, the nonlinear loads absorb the distorted waveform currents. Consequently, they behave like generators of harmonic currents. The circulation of these disturbing currents through the line impedances will cause voltage harmonics and provoke unbalanced voltages. These disturbances will be superimposed on the nominal grid voltage. Various methods have been proposed to detect and to recognize the power quality disturbances in the distribution grid: S-transform and Stockwell's transform method [1], the space vector signature analysis method [2] and identification with artificial neural networks [3] and others. In literature, after detection, recognition and classification of the grid disturbances, different configurations have been applied in order to improve the energy quality supplied to the consumer. It is to compensate all type of disturbance as: voltage and current harmonics, unbalances, reactive power and voltage dips. The conventional passive filter has been traditionally used to improve the power quality of the electrical grid. However, it has several issues such as its bulk, its resonance, fixed filter frequency and difficulty in tuning [4], [5].The parameters and the position of the filter depend strongly on the grid structure. In [6], H. Suyono *et al*. discussed the optimal location and rating of the compensation capacitor bank. They proved that the position of the filter can reduce the active power losses on a transmission line, minimize voltage variation, and improve the voltage stability of the grid. However, the structure of the actual grid becomes a polymorphic structure. Parallel and series active filters configuration and their combination need a supplement control algorithm and an additional investment in the power electronics devices and in the complement power components. The conventional active filter needs the use of the Direct Current (DC) storage device. The Direct Current Bus Capacitor (DCBC) has been proved to be the most failure-prone component in the power electronic circuits. These capacitors are subjected to accelerated failures in hot/arid environments [7] and are attributed to 30% of the failures that occur in power electronics [8]. The energy storage inductors have been proved to be limited by its magnetic saturation and its electromagnetic compatibility (EMC) [9]. The Battery Energy Storage System (BESS) [10] presents an additional investment on the power components and a supplement maintenance cost caused by the Life Cycle Cost (LCC) of the batteries.

Manuscript received March 15, 2020; revised May 30, 2020; accepted June 10, 2020.
Corresponding author: Youssef Ait El Kadi (email: youssefaitelkadiusms@gmail.com).

doi: 10.18178/ijeetc.10.1.36-48

The photovoltaic system filter allows to use the PV DC-bus source rather than the inductive energy storage, electrolytic capacitors or the batteries in addition to the generation and injection of the active power. Moreover, the Active Power Filters (APF) are not efficient when the source voltages are not symmetric [11] or in situations where the load generates the voltage harmonics which are called Harmonic Voltage Source (HVS) loads [12]. The active power filter is based on generating of the current opposite to the load current harmonics. This classic configuration is supplied by a constant voltage source in the DC side. If this DC voltage source is obtained from the same grid then there will cause a pollution of this grid and a return of harmonics generated by this filter itself. The use of photovoltaic (PV) systems to substitute the conventional filter system at different points of the grid proves to be an adequate and efficient solution for all types of disturbances that may appear in the power grid [13], [14]. In [15], the active power filter supplied by the photovoltaic source was used to compensate the harmonics generated by the fixed and balanced nonlinear loads. That reduces the technical and financial constraints of installing a particular active filter. Nevertheless, most of electrical grid disturbances are actually an unavoidable consequence of the increasing use of the unbalanced nonlinear variable loads (single-phase variable speed drives, single-phase motors starters, domestic electronic devices and energy efficient lamps (fluorescent and LED), intermittent renewable energy and Smart grid control devices [16]. For these reasons, this work aims to control a PV-STATCOM connected to the disturbed grid in order to ensure an optimal compensation of the zero-sequence load current and of the harmonic pollution. The compensation of these disturbances generated by the nonlinear unbalanced loads is done in addition to the injection of the active power and the compensation of the request reactive energy.

The paper is organized as follow: Section II details the system configuration and control strategy by presenting the description of the instantaneous power method. The obtained results for different studied scenarios and cases are presented and discussed in Section III. In this section, we evaluate the performances of the studied system in accordance with different situations: System without photovoltaic filter, system with photovoltaic filter under a constant solar radiation, system with photovoltaic filter under a variable solar radiation, variable nonlinear load and unbalanced variable nonlinear loads. The last part of this section presents a comparison of the obtained performances in this study with other control methods published in the literature. Finally, Section IV presents the main conclusion.

II. System Configuration and Control Method

A. System Configuration

The studied configuration consists of a PV solar generator connected to the DC bus of a three-phase voltage inverter. This inverter is connected to the distribution grid low voltage-medium voltage through a choke-inductor. The electrical grid supplies various nonlinear variable loads constituted by the three-phase diode bridge rectifier and thyristor bridge feeding the resistor-inductor series block. Moreover, the same three-phase grid supplies a highly unbalanced variable inductive load at Point of Common Coupling (PCC). The block diagram of the Fig. 1 illustrates the main components of the studied model.

The proposed photovoltaic static compensator (PV-STATCOM) (as described in Fig. 1) is a power electronic configuration based on power active filter device. The DC-bus is linked to the photovoltaic generator rather than to a capacitor. The main building block in the proposed capacitor-less configuration is the photovoltaic station. This configuration allows to generate the active power and to simultaneously supply the three-phase Voltage Source Inverter (VSI) of the filter. The photovoltaic station is a PV array that consists of 66 strings of modules connected in parallel; each string consists of 6 modules connected in series. All modules receive a radiation I_r(W·m^{-2}) under a temperature T(℃). This PV station can generate and supply 120kWc (peak value) to the distribution grid. The module's specifications under standard test conditions STC (irradiance 1000 W·m^{-2}, cell temperature = 25℃) are detailed in Table I. The boost DC-DC converter allows to adapt the PV output voltage to that of the DC bus. This converter is driving by the maximum power point tracking (MPPT) controller.

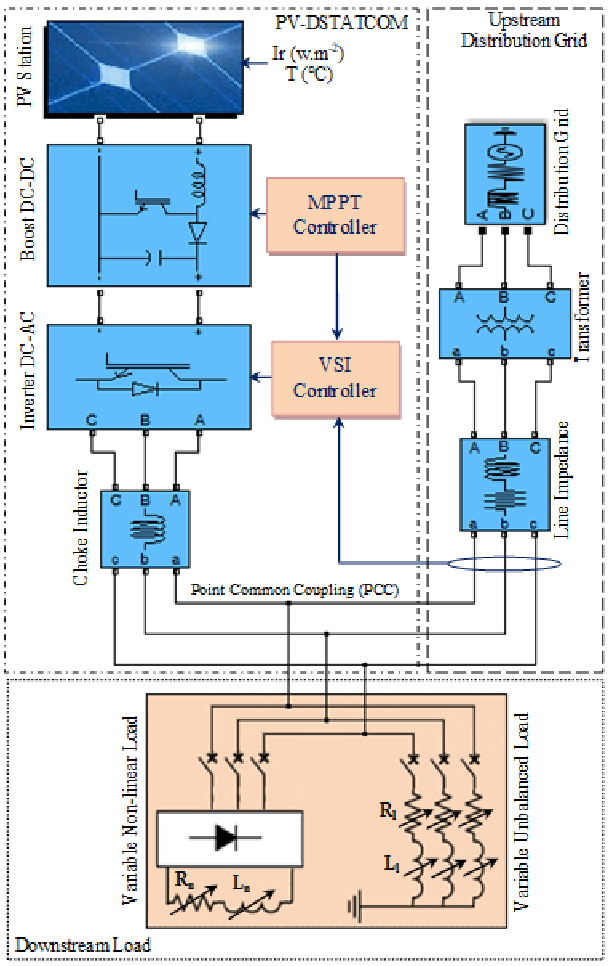

Fig. 1. PV-STATCOM: Studied configuration.

TABLE I: DETAILED SYSTEM SARAMETERS

Parameters	Ratings
PV-Station	Station's structure: - Module type: Sun Power SPR-305-WHT - 6 series-connected modules per string - 96 cells per module - 66 parallel strings Module's specifications under Standard Test Conditions STC (1000 W·m^{-2}, 25 °C): - Short-circuit current I_{SC}=5.96A - Open circuit voltage V_{oc} =64.2V, - Current at maximum power point: I_{mp}=5.58A - Voltage at maximum power point V_{mp}=54.7V - Parallel resistance R_p=993.51Ω - Series resistance R_s=37.998m Ω
Boost DC-DC	U_{max}=750 V , I_{max}= 500A
Voltage Source Inverter VSI	Standard three-phase IGBT based bridge DC interface voltage: 700 V AC interface voltage: 3x380 V- 50Hz
Choke inductor	0.05 mH
Distribution Grid	Medium Voltage Line: 22kV-50Hz-250kVA
Power transformer	22kV/380V-150kVA
Line impedance	0.002 + j 0.251 (Ω)
Unbalanced load	Variable resistor and variable inductor
Variable Non- linear Load	Three-phase diode bridge rectifier with variable resistor and variable inductor load

The Voltage Source Inverter (VSI) links the PV station to the distribution grid at the point of common coupling (PCC) through the choke inductor and the bus bars as shown in Fig. 1. The VSI generates 380V-50Hz which is stepped up to 22kV using 22kV/380V power transformer for distribution grid. Upstream, toward the substation, is modeled as a three-phase distribution grid 22kV-50Hz-250kVA and a power transformer 22kV/380V-150kVA with series line impedance (Z_l). Downstream is modeled as two blocks. The first one is the harmonics generator block. This block is constituted by three-phase diode bridge rectifier feeding a variable resistor-inductor series block R_n-L_n. It will generate harmonic currents that represent the aggregate behavior of harmonics producing loads such as variable speed drives, motors starters for pumps, frequency converters, electronic devices supplies and energy efficient lamps (fluorescent and LED), etc. The second block is the variable unbalanced loads that are lumped into equivalent resistor inductor R_l-L_l as shown in Fig. 2. These variable and unbalanced loads absorb the reactive and active energy and generate the zero-sequence component and the harmonics pollution. The Voltage Source Inverter (VSI) controller is based on the instantaneous powers with current control method. The specification of this control method will be detailed at the end of this section. Table I. summarizes the specifications of the proposed photovoltaic STATCOM.

B. Control Method

The energy flow is examined in various regimes imposed by the fluctuation of the radiation level and the variation of the unbalanced nonlinear load. It should be noted that, with the used configuration, the material investment is identical to that of a conventional photovoltaic installation connected to the grid without any additional devices and costs. To improve the quality of the energy at the point of connection, we just have to add the functionalities of an active filter to the algorithm of the boost DC converter controller and that of the voltage inverter. That allows to ensure simultaneously: the compensation of harmonic pollution, the reactive power, load unbalances, dips voltage and the injection of the active power supplied by the PV station.

Two strategies of control are possible: the follow-up of set-point and the rejection of disturbances [17]. According to the type of signal used for pulse generation, these strategies can be divided into three major families: Instantaneous voltage controller [18], Instantaneous power and current control technique [19], [20]. Among the methods used to determinate the harmonic currents to be compensated, the method of instantaneous power is used in this work. This method is very widespread and simple to implement. The control of the Direct Current-Alternative Current (DC-AC) inverter by the instantaneous power method is robust [21]; According to various conditions imposed by the fluctuation of solar radiation and the variation of the nonlinear load, an analysis of the powers transits is effectuated on the photovoltaic source, on the load and on the grid [20].

The first stage is to convert the primary real voltages v_a, v_b, v_c, and currents i_a, i_b, i_c to the two-phase (α, β) reference plane by using the Concordia's transformation:

$$\begin{bmatrix} V_\alpha \\ V_\beta \end{bmatrix} = \sqrt{\frac{2}{3}} \begin{bmatrix} 1 & -\frac{1}{2} & -\frac{1}{2} \\ 0 & \frac{\sqrt{3}}{2} & -\frac{\sqrt{3}}{2} \end{bmatrix} \begin{bmatrix} v_a \\ v_b \\ v_c \end{bmatrix} \tag{1}$$

$$\begin{bmatrix} I_\alpha \\ I_\beta \end{bmatrix} = \sqrt{\frac{2}{3}} \begin{bmatrix} 1 & -\frac{1}{2} & -\frac{1}{2} \\ 0 & \frac{\sqrt{3}}{2} & -\frac{\sqrt{3}}{2} \end{bmatrix} \begin{bmatrix} i_a \\ i_b \\ i_c \end{bmatrix} \tag{2}$$

v_a, v_b, v_c and i_a, i_b, i_c: real component of voltage (V) and current (A). V_α, v_β, and i_α, i_β: voltage (V) and current (A) in the two-phase (α, β).

According to (1) and (2), the instantaneous active power p and reactive q are calculated by:

$$\begin{bmatrix} p \\ q \end{bmatrix} = \begin{bmatrix} V_\alpha & V_\beta \\ -V_\beta & V_\alpha \end{bmatrix} \begin{bmatrix} I_\alpha \\ I_\beta \end{bmatrix} \tag{3}$$

These instantaneous powers p (W) and q (VAR) can be divided into two components: The direct continuous component related to the fundamental components ($\bar{p}$, $\bar{q}$) and the alternative component related to the harmonics ($\tilde{p}$, $\tilde{q}$) as following:

$$\begin{cases} p = \bar{p} + \tilde{p} \\ q = \bar{q} + \tilde{q} \end{cases} \tag{4}$$

After that, a power filter is used to separate the harmonic's power component from the fundamental power component. After the separation of these components, the disturbing currents in the reference plane α, β are calculated by using (3) and (4). This technique allows to compensate the reactive energy. In fact, the reactive power's absorption is a result of a non-zero continuous component ($\bar{i}_\alpha$) along the axis α . The filter's current, which allows to compensate simultaneously the reactive power and the whole harmonics, is therefore:

$$\begin{bmatrix} I_{\alpha\_\text{ref}} \\ I_{\beta\_\text{ref}} \end{bmatrix} = \frac{1}{\Delta} \begin{bmatrix} V_\alpha & -V_\beta \\ V_\beta & V_\alpha \end{bmatrix} \begin{bmatrix} \bar{P} - \tilde{p} \\ -\bar{q} - \tilde{q} \end{bmatrix} \tag{5}$$

where

$$\Delta = V_\alpha^2 + V_\beta^2 \tag{6}$$

In the (α, β) axis plane, it is possible to express the current with three components: the active current I_{ref_a}, the fundamental reactive current I_{ref_a} and the set of other harmonics I_{ref_h}:

$$\begin{bmatrix} I_{\alpha\text{ref}} \\ I_{\beta\text{ref}} \end{bmatrix} = \begin{bmatrix} I_{\alpha\text{ref}\_a} \\ I_{\beta\text{ref}\_a} \end{bmatrix} + \begin{bmatrix} I_{\alpha\text{ref}\_r} \\ I_{\beta\text{ref}\_r} \end{bmatrix} + \begin{bmatrix} I_{\alpha\text{ref}\_h} \\ I_{\beta\text{ref}\_h} \end{bmatrix} \tag{7}$$

Active current:

$$\begin{bmatrix} I_{\text{ref}\_a} \end{bmatrix} = \begin{bmatrix} I_{\alpha\text{ref}\_a} \\ I_{\beta\text{ref}\_a} \end{bmatrix} = \frac{1}{\Delta} \begin{bmatrix} V_\alpha & -V_\beta \\ V_\beta & V_\alpha \end{bmatrix} \begin{bmatrix} \bar{p} \\ 0 \end{bmatrix} \tag{8}$$

Reactive current:

$$\begin{bmatrix} I_{ref\_r} \end{bmatrix} = \begin{bmatrix} I_{\alpha ref\_r} \\ I_{\beta ref\_r} \end{bmatrix} = \frac{1}{\Delta} \begin{bmatrix} V_\alpha & -V_\beta \\ V_\beta & V_\alpha \end{bmatrix} \begin{bmatrix} 0 \\ -\bar{q} \end{bmatrix} \tag{9}$$

Harmonic current:

$$\begin{bmatrix} I_{\text{ref}\_h} \end{bmatrix} = \begin{bmatrix} I_{\alpha\text{ref}\_h} \\ I_{\beta\text{ref}\_h} \end{bmatrix} = \frac{1}{\Delta} \begin{bmatrix} V_\alpha & -V_\beta \\ V_\beta & V_\alpha \end{bmatrix} \begin{bmatrix} -\tilde{p} \\ -\tilde{q} \end{bmatrix} \tag{10}$$

The three-phase polluting currents, referred as reference currents I_{ref}, are calculated from the Concordia's inverse transform.

$$\begin{bmatrix} I_{a\_\text{ref}} \\ I_{b\_\text{ref}} \\ I_{c\_\text{ref}} \end{bmatrix} = \sqrt{\frac{2}{3}} \begin{bmatrix} 1 & 0 \\ -\frac{1}{2} & \frac{\sqrt{3}}{2} \\ -\frac{1}{2} & -\frac{\sqrt{3}}{2} \end{bmatrix} \begin{bmatrix} I_{\alpha\_\text{ref}} \\ I_{\beta\_\text{ref}} \end{bmatrix} \tag{11}$$

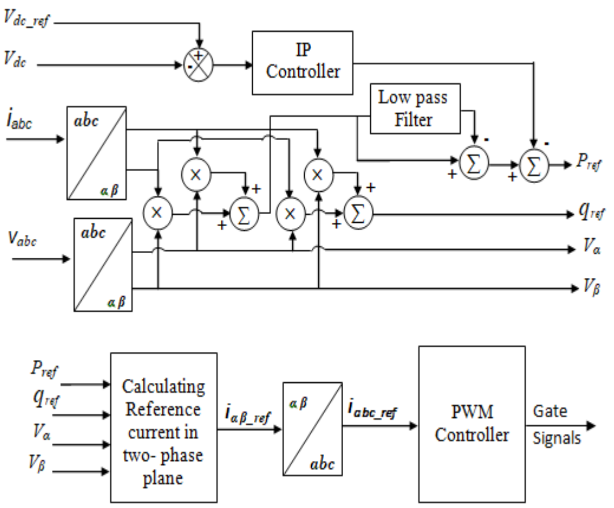

Fig. 2. Instantaneous power and current control: Main diagram [15].

Fig. 2 shows the schematic diagram of the control method. This diagram illustrates the specification of the proposed control strategy of the photovoltaic filter system. The references of the currents to be injected by the active filter are controlled in the two-phase plane "α, β" by using the current control strategy. In Fig. 2, the first blocks allow to calculate the voltage and current components I_α, I_β and V_α, V_β with Concordia's matrix in terms of the real components i_a, i_b, i_c and v_a, v_b, v_c in (1) and (2). The control method is based on determination of the harmonic currents to be compensated by using the instantaneous power method. The harmonic references $i_{\alpha\text{-ref}}$ and $i_{\beta\text{-ref}}$ are extracted from the instantaneous power active p and reactive q in the plane "α, β". For internal loop, (i.e. the current's loop in the Pulse Wide Modulation (PWM) block), a Proportional Integral Derivate (PID) controller is used in order to force the supplied filter currents to follow quickly their references. Concerning the external loop, (loop of the DC bus voltage), an Integral Proportional (IP) controller is used to keep the DC voltage V_{dc} at its set-point value. The compensated error in the IP controller's output is then added to the current reference in the α axis. The control of the PV-STATCOM is done by two controllers; the PI controller regulates the DC-link voltage, the PID controller allows to the inverter to produce the opposite polluting currents to be compensate. The output of IP controller is deducted from the active power reference P_{ref}. After that, we calculate the reference active currents to be generated by the PV-STATCOM.

For the Integral Proportional (IP) controller and the Proportional Integral Derivative (PID) tuning, the parameters depend on the transfer function of the plant to be controlled. Since it is difficult to know the transfer function of the global system, the heuristic Ziegler-Nichols method is used to tune the parameter of the both controller IP and PID. The parameters of the IP controller (proportional and integral constants) are determined according to specific criteria (like steady error, overshoot and large stability margin). The proportional gain, integral and derivative gains of the PID controller are adjusted in order to ensure a fast dynamic and a settling time of the inverter. This fast dynamic allows to follow the fast variation of the disturbing current.

III. Results and Discussion

A. System without Compensation

In a first stage, the system operates without compensation filter. The grid supplies to the nonlinear loads an active power equal to 20kW and a reactive power equal to 15kVAR. The curve of the grid current is shown in Fig. 3, the current is characterized by a shape distortion. The waveform of the fundamental component is delayed from that of the voltage grid; a reactive power is provided by the grid.

Fig. 4 shows a frequency spectrum of the grid current. It contains pair-order and odd-order harmonics. The first odd-order harmonics (no-multiple of 3 i.e. 5, 7, 11, 17) have a high amplitude. The primary effect of these harmonics is an increase in the iron and copper losses, thus the additional heat generated. Voltage distortion increase losses due to hysteresis and eddy currents and causes overstressing of the insulation material used. Without connecting the PV-STATCOM device, the Total Harmonic Distortion value is: THD=28.80%.

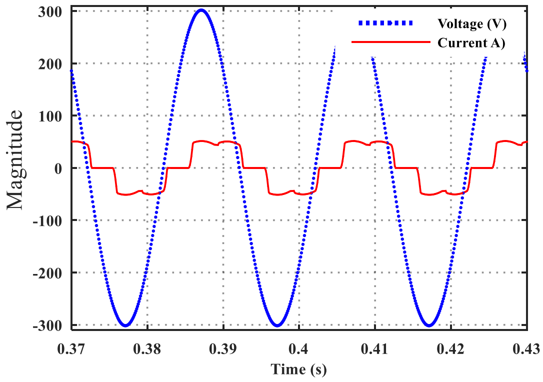

Fig. 3. Voltage and grid current waveform without compensation.

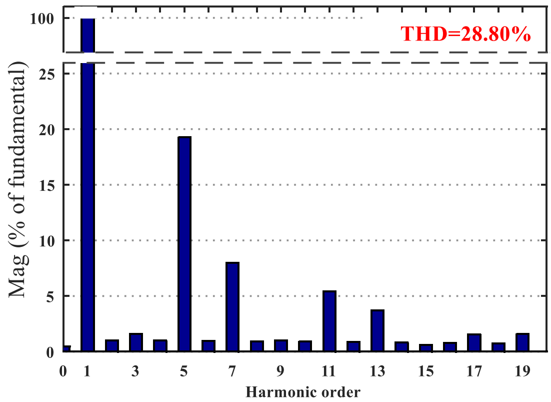

Fig. 4. Current harmonics orders and grid THD without connecting PV-STATCOM.

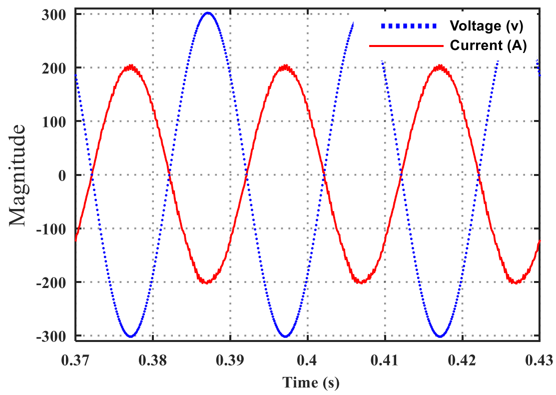

Fig. 5. Voltage and grid current waveform with PV-STATCOM under constant radiation.

B. System with Photovoltaic Filter under a Constant Solar Radiation

In this second case, the photovoltaic filter (PV-STATCOM is connected to the grid. The temperature and the radiation level are fixed at standard conditions (T_{co}=25°C, E_{co}=1000W·m^{-2}). The grid supplies the nonlinear load constituted by the three-phase diode bridge rectifier bridge feeding the resistor-inductor series block which absorbs an active power equal to 20kW and reactive power equal to 15kVAR. In Fig. 5, the opposite phases between the voltage and current waveforms prove the injection of the excess active energy produced by the PV-STACOM into the distribution grid.

As shown in Fig. 6, the Total Harmonic Distortion (THD) of the grid current is significantly improved; the THD value is reduced to 2.02% by connecting the PV-STATCOM device and this is a remarkable improvement of the energy quality supplied into the distribution grid. A power consumption reduction will be realized by eliminating harmonic currents. The greatest benefits will be achieved on the devices life cycle with harmonic mitigation: smooth-running of protection equipment, under-loading of cables and transformers.

C. System with Photovoltaic Filter under a Variable Solar Radiation

In the literature, the daily average radiation for each calendar month on surfaces facing directly towards the equator has been presented by Liu and Jordan [22]. Fig. 7 presents the global hourly solar radiation incident on inclined surfaces with an inclination value equal to the latitude of the considered the photovoltaic (PV) station [23], [24]. Fig. 7 shows the variation of the solar irradiance, on real time, from sunrise to sunset on the summer solstice and the winter solstice days. The location coordinates of the PV-station (case of Noor Ouarzazate Solar Complex, Morocco) are: Latitude 30°59′40″ N, Longitude 6°51′48″ W, Altitude=1200 m.

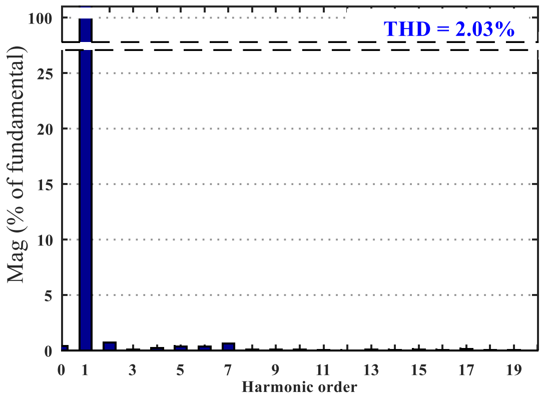

Fig. 6. Harmonics of the grid current with PV-STATCOM under constant radiation.

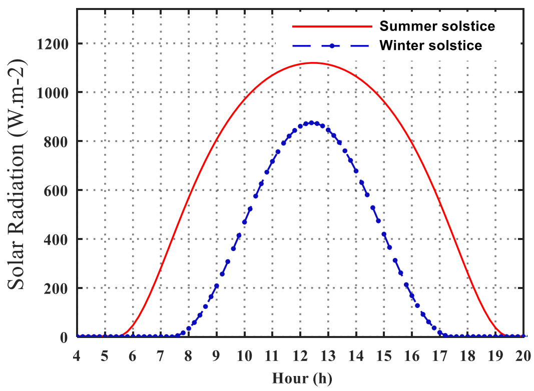

Fig. 7. Global solar radiation on June 21st and December 21st

The radiation variation on photovoltaic panels is due to the deterministic periodic events on one hand (sunrise and sunset) as shown in Fig. 7, and to the pseudo-random phenomena on the other hand. These pseudo-random phenomena are due to the weather conditions (climate change, clouds) or environmental (transitional shading, dust settlement, etc.).

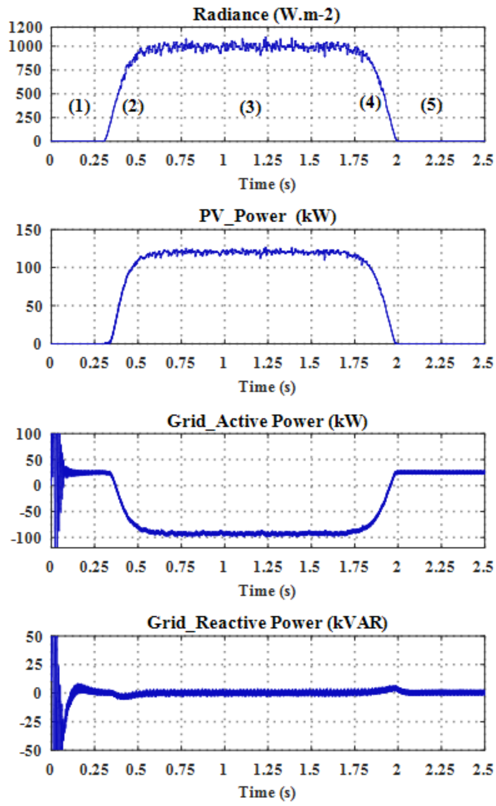

Fig. 8. Instantaneous powers during a cycle of variable solar radiation.

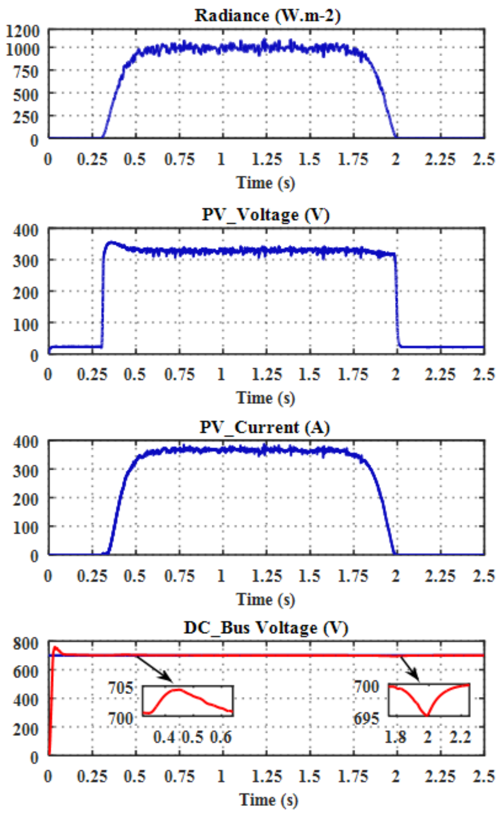

Fig. 9. Evolution of voltage and current of the PV-station.

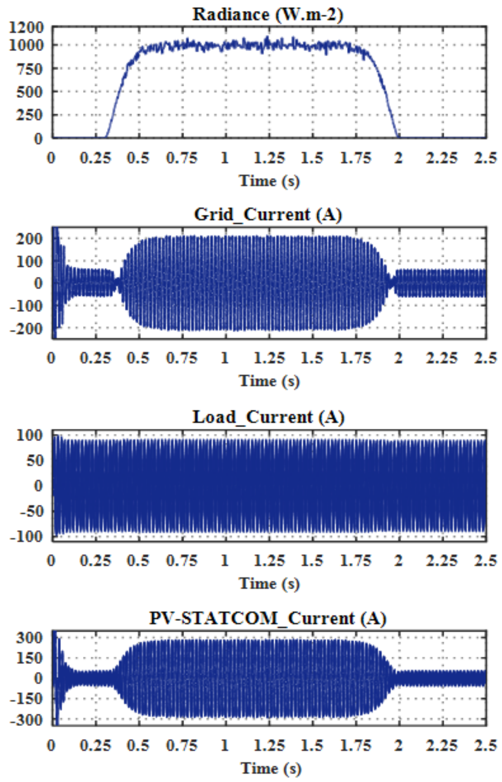

Fig. 10. Evolution of the currents of grid, load, and filter.

To assess the performance of PV-STATCOM in view of these variations, the photovoltaic panels receive a variable solar radiation as shown in Fig. 8. During a daily cycle of solar variable radiation, Fig. 8, Fig. 9, and Fig. 10 illustrate the evolution of the photovoltaic voltage, photovoltaic current and instantaneous active and reactive grid powers. The variable radiation describes (in reduced time) the periods of darkness (zone 1 and 5), the sunrise and sunset time (zone 2 and 4), and the constant radiation phase (zone 3).

The constant radiation is superimposed with Gaussian noise in order to simulate the case of the presence of pseudo-random variations caused by the climate change and the environmental conditions. For a non-zero solar radiation, the PV-STATCOM products the active power and supplies the load and the grid. After a transient regime necessary for the stability of the system between (0s to 0.12s), there is no exchange of reactive power between the grid and the nonlinear inductor load; the latter is completely compensated by the filter. During the darkness period, the station compensates the reactive energy.

Fig. 9 shows that after the transient state (after 0.12 s), the DC-bus voltage still stable except a small variation ($\approx \pm 5$V) at the time of the high variation of the radiation (during sunrise and sunset).

Fig. 11 illustrates the improvement of the Total Harmonic Distortion (THD) of the distribution grid. Under a non-zero value of radiation, the PV-STATACOM reduces the THD from value 41.5% to 2.02%. The THD curve also shows the abrupt peaks that appear at the moments of equality of the power provided by the PV station with the load's power (at 0.39 s and at 1.92 s). At these moments, the power supplied by the grid is zero; the fundamental current tends towards zero, hence the THD increases.

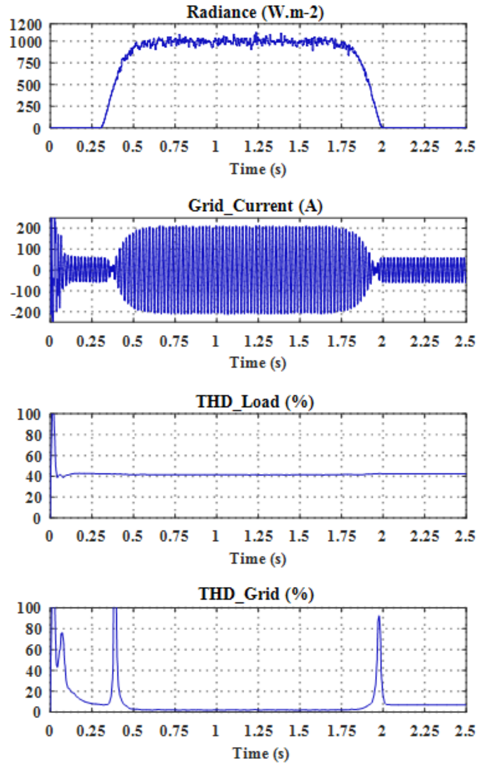

Fig. 11. Evolution of the THD of the load and the grid.

TABLE II: TRANSIENT PERFORMANCES UNDER VARIABLE RADIATION

Transient convergence time (ms)	
DC-bus voltage	60 ms
THD of the load current	40 ms
THD of the grid current	120 ms
Settling time of DC-bus voltage (ms)	
During increasing of the radiation (sunrise)	300 ms
During decreasing of the radiation (sunset)	350 ms
DC-bus voltage variation (%)	
During increasing of the radiation (sunrise)	+0.63%
During decreasing of the radiation (sunset)	-0.67%

TABLE III: STEADY STATE PERFORMANCE CHARACTERISTICS UNDER VARIABLE RADIATION

	THD Load (%)	THD Grid (%)	THD Improvement rate (%)	DC-bus Voltage (V)
Before sunrise	42.42	7.04	83.76	700.50
After sunrise	41.40	2.02	95.13	699.55
Before sunset	41.44	2.04	95.08	699.80
After sunset	42.43	6.92	83.69	700.32

Table II and Table III summarize the performance characteristics of the PV-STATCOM when it receives a variable radiation (cases of the sunrise and sunset conditions). The results prove a good behavior of the PV-STATCOM in the transient and the Steady state. Table IV shows the evolution of THD, the active and reactive powers of the PV-STATCOM under variable radiation.

For fairly sufficient radiation values, the PV-STATCOM compensates harmonics and reactive energy, and keeps supplying the active energy to the grid. The value of Total Harmonic Distortion remains reduced and stable. That proves the robustness and reliability of the compensation station under variable radiation. Moreover, the DC bus voltage remains almost stable and equal to its reference value (≈700V). That shows a weak influence of disturbances on the station. For low radiation values, the THD starts to increase, but the station continues to compensate the reactive energy.

TABLE IV: PERFORMANCE MEASUREMENTS UNDER VARIABLE RADIATION

Radiation ($W \cdot m^{-2}$)	DC bus voltage (V)	THD (%)	Reactive power (kVAR)	Active power (kW)
1073	698.399	1.954	0.215	-94.306
1035	702,590	2,042	-0,313	-95,669
1021	701.034	2.024	2.709	-93.427
1016	701,670	2,022	0,199	-93,359
1008	701.105	1.963	-1.960	-96.636
1000	702,195	2,035	-0,069	-90,874
980	702,181	2,031	-0,099	-92,029
972	701,422	2,205	-0,017	-89,846
965	698.911	1.963	1.435	-89.788
960	702,350	2,021	-0,151	-87,695
940	702,004	2,087	-0,143	-83,406
880	700,764	2,807	0,447	-79,987
785	700.009	2.954	0.966	-70.740
80	699,957	6,485	-0,057	27,362
0	699,557	6,485	-0,022	28,058

D. Photovoltaic Filter with Variable Nonlinear Load

In this case, the photovoltaic filter connected to the grid supplies a variable nonlinear load. The objective is to evaluate the behavior of the PV-STATCOM and the robustness of the control algorithm after abrupt and spontaneous variations of the nonlinear loads. These variations are either in type or in the value of the load.

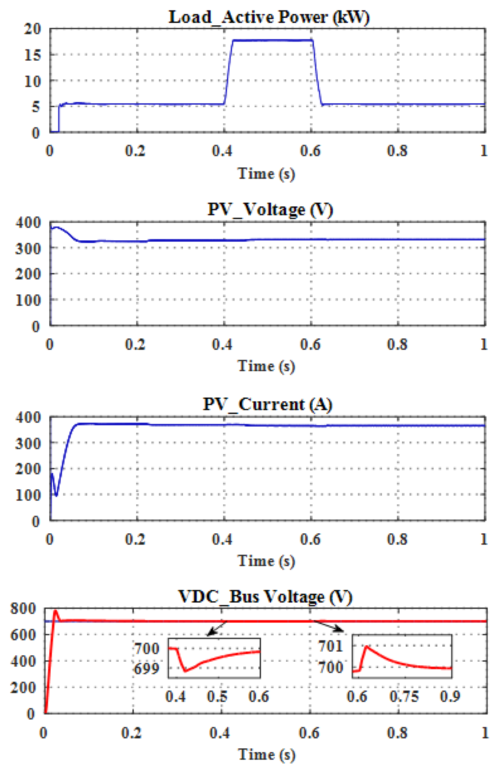

Fig. 12. PV-Station voltage and current with an abrupt variation of the nonlinear load.

Fig. 12 shows the evolution of the photovoltaic voltage and current before and after an abrupt variation of the nonlinear load. The time of the disturbance is localized between (0.4s to 0.6s). We observe that the variation of the load doesn't have any effect on the DC bus voltage, the last remains stable during steady-state (V_{dc}≈700V). That proves the ability of the used control method to minimize the effect of the filter on the PV station.

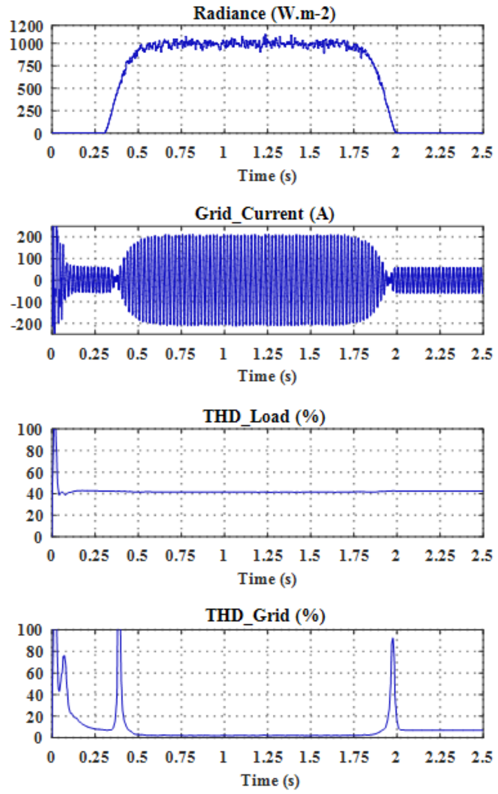

Fig. 13. Active and reactive grid power in the case of an abrupt variation of the nonlinear load.

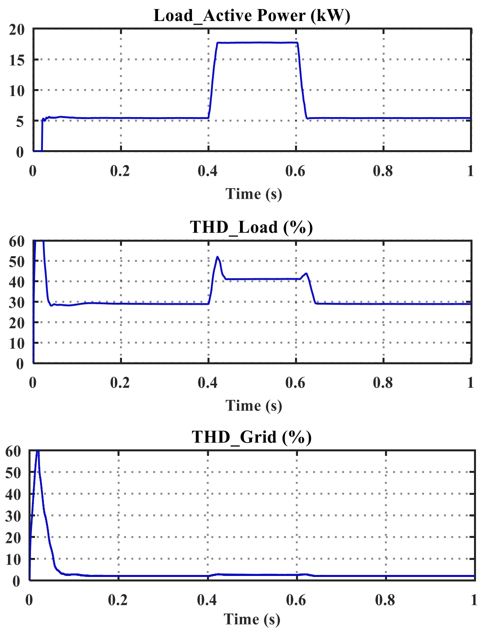

Fig. 14. Evolution of the grid-THD in the case of an abrupt variation of the nonlinear load.

Fig. 13 shows that the PV-STATCOM allows to compensate the reactive power even in the case of an abrupt variations of the nonlinear load. Despite the variation of the reactive load power from 7.50kVAR to 11kVAR, the PV-STATCOM compensates all reactive energies and the reactive grid power remains zero. Fig. 14 presents the evolution of the grid-THD in the case of an abrupt variation of the nonlinear load.

In Fig. 14, the abrupt variation of the nonlinear load appears at 0.4s, it provokes a sudden increase of the THD of the load current from 28.81% to 41.15%. The photovoltaic filter limits the THD of the grid current at 2.57%. That proves the efficiency of the control method even when the nonlinear load varies. This variation of THD (from 2.03% to 2.57%) is due to the variation of the operating point of the nonlinear system. Fig. 15 presents the load and the grid current forms. It shows that the PV-STATCOM keeps the sinusoidal waveform of the grid current even if nonlinear load changes.

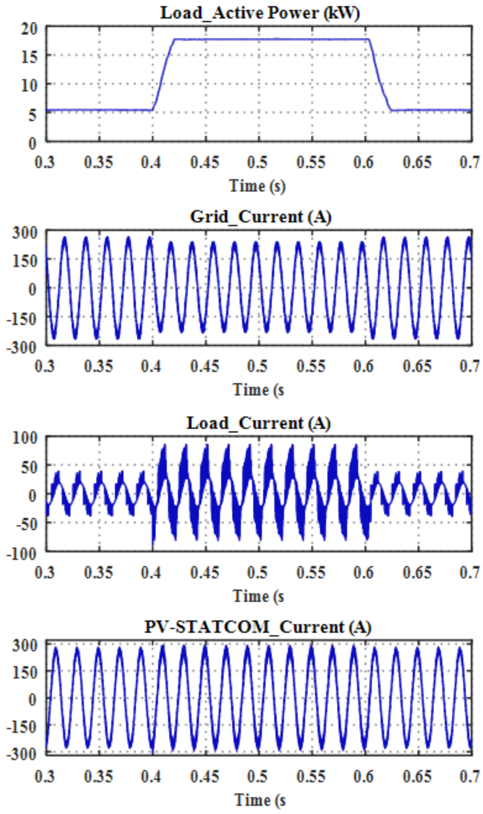

Fig. 15. Grid, load and PV-STATCOM currents before and after abrupt variation of the unbalanced nonlinear load.

TABLE V: TRANSIENT PERFORMANCE CHARACTERISTICS WITH VARIABLE NONLINEAR LOAD

Transient convergence time (ms)	
DC-bus voltage	60 ms
THD of the load current	40 ms
THD of the grid current	120 ms
Settling time (ms)	
DC-bus voltage	250 ms
THD of the load current	40 ms
THD of the grid current	40 ms
DC-bus voltage variation (%)	
After connection of the nonlinear load	-0.16%
After disconnection of the nonlinear load	+0.17%

Table V and Table VI summarize the performance characteristics of the Total Distortion Harmonic and that of the DC-bus voltage. Despite the nonlinear variable loads, the PV-STATCOM proves a fast dynamic less than 250 ms in the transient state, and keeps a large stability level of the DC-bus voltage. The improvement rate of the THD stills more than 92.95% in the steady state.

TABLE VI: STEADY STATE PERFORMANCE CHARACTERISTICS WITH VARIABLE NONLINEAR LOAD

	THD Load (%)	THD Grid (%)	THD improvement rate (%)	DC-bus Voltage (V)
Before nonlinear load connection	28.81	2.03	92.95	699.97
After nonlinear load connection	41.15	2.57	93.75	699.80
Before nonlinear load disconnection	41.05	2.55	93.79	699.60
After nonlinear load disconnection	28.89	2.06%	92.87 %	699.92

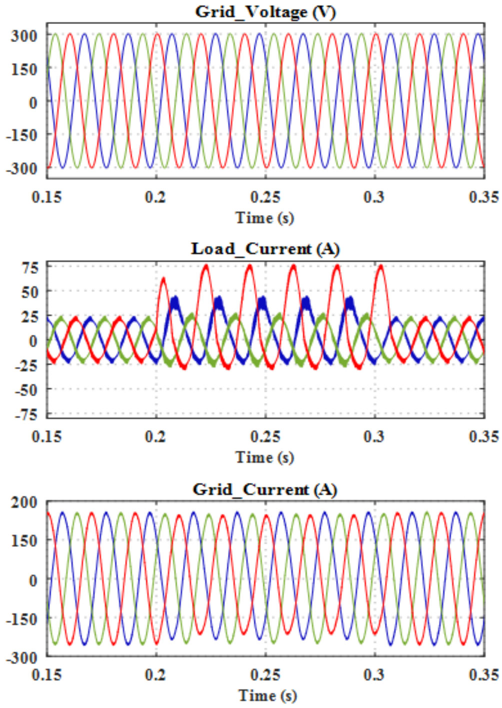

Fig. 16. Waveforms of load and grid currents before and after abrupt variation of the unbalanced nonlinear load.

E. Photovoltaic Filter with Unbalanced Variable Nonlinear Load

In this latter case, various unbalanced three-phase loads are connected to the output of the photovoltaic filter connected to the grid. Fig. 16 presents the waveforms of the grid voltages, the load currents, and grid currents. The unbalanced load is supplied between 0.2s and 0.3s. The three-phase load currents become unbalanced as shown in Fig. 16.

The aim is to evaluate the capacity of the PV-STATCOM to compensate the unbalanced components (positive, negative, and zero-sequence components of three-phase voltages and currents) of the load currents and to restore the balance of the grid currents. Fig. 17 presents the evolution of the zero-sequence component of the load and the grid currents and their THD. At the moment of the appearance of an unbalance load (at 0.2s), the zero-sequence component of the load currents (I_{o_load}) increases from 0 to 31.50%. The THD of the load currents rises from 7.5% to 22.80%. However the photovoltaic filter connected to the grid limits this zero-sequence component of the grid current (I_{o_grid}) at 4.26 % (Fig. 17) and keeps the THD of the grid currents under 3.10 %. These advantageous effects remain acceptable according to IEEE 929 and IEEE 1547 standards.

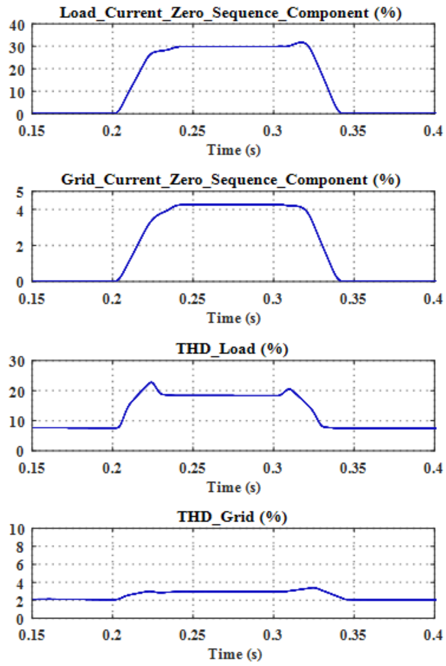

Fig. 17. Evolution of the zero-sequence component and THD of grid current before and after abrupt variation of unbalanced nonlinear load.

TABLE VII: TRANSIENT PERFORMANCE WITH VARIABLE UNBALANCED NONLINEAR LOAD

Transient convergence time (ms)	
THD of the load current	40 ms
THD of the grid current	120 ms
Zero-sequence component of load current	20 ms
Zero- sequence component of grid current	20 ms
Settling time (ms)	
THD of the load current	20 ms
THD of the grid current	25 ms
Zero-sequence component of load current	40 ms
Zero- sequence component of grid current	40 ms

TABLE VIII: STEADY STATE PERFORMANCE CHARACTERISTICS WITH VARIABLE UNBALANCED NONLINEAR LOAD

Before connection of the nonlinear unbalanced load	
THD of the load current	7.50%
THD of the grid current	2.10%
THD improvement rate (%)	72%
After connection of the nonlinear unbalanced load	
THD of the load current	22.80%
THD of the grid current	3.10%
THD improvement rate (%)	86.40%
Zero-sequence component of load current	31.50%
Zero- sequence component of grid current	4.26%
Balanced improvement rate (%)	86.48%

Table VII and Table VIII present the performance characteristics of the PV-STATCOM in the case of the nonlinear unbalanced loads are supplied. After connection of the nonlinear unbalanced loads, the THD of the load increases from 28.81% to 41.15%. Despite this load distortion, the PV-STATCOM keeps the THD of the grid less than 2.57%. Therefore, the improvement rate of THD is equal to 86.40 %. The zero- sequence component of the grid currents is reduced from 31.50 % to 4.26 %; that means an improvement rate equal to 86.48 %. These results prove the ability of the PV-STATCOM to restore the balance of the grid currents in spite of the unbalanced three-phase variable loads.

F. Synthesis and Comparaison of Results

To improve efficiently the power quality in distribution grid, three main objectives should be achieved [2]:

- Assess the impact of the harmonic grid currents and reduce the THD according to the guideline specified in the International standard requirement as per International Electro-technical Commission (IEC) standard.
- Good dynamic response and fast convergence of the control algorithms allowing to follow the abrupt disturbances. These disturbances are caused by the fast power electronic equipments generating of disturbances and itself influenced by these disturbances.
- Ensure the stability of the parameters of the actual polymorphic grid structures, as well as the strong trend towards bidirectional exchange grid including the intermittent renewable energy sources [25].

Different analysis and techniques control have been developed in the literature. All methods used to improve the power quality have their own advantages and disadvantages.

- In [26], Rahmani *et al*. used the nonlinear control technique with computational control delay compensation to control a three-phase shunt active power filter with DC link capacitor. The nonlinear load was constituted by a three-phase diode bridge rectifier with resistor and inductor load. The authors declared a good dynamic response and DC-link voltage variation of 3.5%. The THD of the grid current was reduced from 14% before compensation to 3.1% after compensation.
- In [27], the authors used the discrete Proportional Integral (PI) and hysteresis control scheme to filter the harmonics in a distribution grid connected to a wind energy generation system. The THD was reduced from 27% to 3.04%.
- References [28] and [29] studied a compensator based on adaptive filter control. This method was based on adaptive nature for synchronous extraction in the time domain for deriving reference supplied currents. It was applied under distorted alternative current feeding to three-phase linear and nonlinear loads. The transient performance of this method shows a dynamic performance of 0.6 sec. The THD of the load current and the grid current are respectively 25.34% and 2.84%.
- In [30], M. Mahdianpoor *et al*. used the Proportional-Resonant (PR) controller. The studied filter consisted of an injection transformer, an inverter output filter, a voltage source converter and a DC-link capacitor. The authors confirm a reduction of the THD from 21.7% before compensation to 5.83% after compensation.
- In [10], J. Hussain *et al*. introduced the power quality improvement technique of disturbed grid using STATCOM with Battery Energy Storage System (BESS). The THD without compensation was 4.94%. With the STATCOM, the THD became 1.32%, the stability of the system was been achieved after 2 sec. However, the use of the BESS presents an additional investment on power components and a supplement maintenance cost caused by the Life Cycle Cost (LCC) of the batteries.
- In [9], W. Rohouma *et al*. studied harmonics compensation in a distribution grid. The proposed strategy is based on a Matrix Converter (MC) which was controlled using Finite Control Set Model Predictive Control (FCSMPC). This approach used the inductive energy storage rather than electrolytic DC-Bus capacitors. The authors proved the reduction of the currents THD from 26.99% to 3.43%. However, this adds additional complexity and cost in addition to the magnetic saturation and the electromagnetic compatibility problems.

In this study we use the current control and identification of harmonic currents by the instantaneous power method. Table IX summarizes the comparison of the dynamic response, the harmonic distortion rate and other performances obtained with other control methods published in the literature.

According to Table IX, The performances of the studied photovoltaic PV-STATCOM based on the current control algorithm with instantaneous power are demonstrated. This compensation method is efficient for harmonics elimination and DC-Bus Voltage stabilization. It ensures too a good dynamic response. The THD is significantly improved from 28.81% to 2.03% then a reduction rate equal to 92.98%. The DC-Bus voltage of the PV-STATCOM is also regulated to the desired value despite the varying load and irradiance conditions. These results confirm the capability of the presented Photovoltaic STATCOM to improve the power quality of distribution grid without any additional devices and costs, but only by integration of the functionalities of an active filter in the photovoltaic inverter controller.

TABLE IX: COMPARISON DIFFERENT CONTROL CHARTS PUBLISHED IN THE LITERATURE

Control strategy	THD value			DC-Bus Voltage stabilization	Dynamic Response	Additional devices cost
	Without Compensation	After compensation	Reduction Ratio			
Nonlinear control technique with computational control delay compensation *S. Rahmani et al. [26] (2010)*	14%	3.1%	77,86%	3.5%	75ms	Voltage source inverter (VSI), DC-side Capacitor, AC-side high-frequency inductors

Control strategy	THD value			DC-Bus Voltage stabilization	Dynamic Response	Additional devices cost
	Without Compensation	After compensation	Reduction Ratio			
Discrete Proportional Integral (PI) and hysteresis control. *M. Ravindra et al. [27] (2012)*	27%	3.04%	88,74%	--	150 ms	Voltage source inverter (VSI), DC energy storage capacitor
Compensator based on adaptive filter strategy N. Narasimhulu *et al* [28] (2016) *R. M. Reddy et al. [29] (2018)*	25.34%	2.84%	88,79%	30%	600 ms	VSI, DC bus capacitor, Interfacing inductors, Ripple filters: R-C
Proportional-Resonant (PR) controller *M. MAHDIANPOOR et al. [30] (2017)*	21.7%	5.83%	73,13%	--	---	Injection transformer, Inverter output filter, Voltage source converter (VSC), DC-link capacitor
STATCOM with battery energy storage system (BESS) *J. Hussain et al. [10] (2019)*	4.94%	1.32%	73,28%	--	2 s	Injection set-down transformer, Voltage source converter (VSC), Batteries
Matrix converter (MC) with finite control set model predictive control (FCSMPC) *W. Rohouma et al. [9] (2019)*	26.99%	3.43%	87.29%	--	100 ms	Three-phase matrix converter (18 IGBT modules SK60GM123 - 18 power diodes), Clamp circuit (2 three-phase diode bridge rectifier), Three-phase input filter R-L, -Output chokes Inductors
Current control with instantaneous powers *This work*	28.81%	2.03%	92,95%	< 0.67 %	40 ms	Any additional device except that already used in photovoltaic production

IV. Conclusion

The PV-STATCOM connected to the distribution grid can ensure, in addition to the production and injection of the active power, an optimal compensation of the all grid disturbances. The performances of photovoltaic filter are modeled and evaluated with the use of the instantaneous powers theory and DC voltage reference control under variable weather environment and load conditions. This compensator improves the THD as well as it compensates the reactive energy and the zero-sequence component of the load currents. This compensation stills efficient despite the variable radiation, variable and unbalanced nonlinear loads. The control algorithm eliminates the harmonics and maintains the Total Harmonic Distortion limit according to IEEE 929 and IEEE 1547 standards.

Moreover, the used control algorithm is easy to be implemented because of its simplicity and it needs less computational time. The efficiency of the control algorithms is verified. Indeed, the results show the robustness of the control technique based on the identification of the disturbances by using the instantaneous power method instead of the frequency method which requires a high computation time. This method allows a better control of the instantaneous active and reactive powers, as well as a significant improvement of the THD. In addition to that, the studied system allows to restore the balance of the grid currents in spite of the unbalanced three-phase variable loads. The studied PV-STATACOM is an efficient solution to improve the energy quality in the distribution grid.

Conflict of Interest

The submitted work was carried out without any conflict of interest. The authors declare no conflict of interest.

Author Contributions

Y. Ait El Kadi conducted the research and wrote the paper. Y. Lakhal prepared the program code. F. Z. Baghli analyzed the results with Y. Ait El Kadi; the final revision is completed by the three authors; all authors had approved this final version.

Acknowledgment

The authors are sincerely grateful to thank all members of the Laboratory of Engineering and Applied Technologies of Sultan Moulay Slimane University.

References

[1] S. J. Alqam and F. R. Zaro "Power quality detection and classification using s-transform and rule based decision tree", *International Journal of Electrical and Electronic Engineering & Telecommunications*, vol. 8, no. 1, pp. 45-50, January 2019.

[2] Y. A. El Kadi, F. Z. Baghli, and Y. Lakhal, "Energy quality optimization in smart grids faults monitoring by the space vector signature analysis method" in *Proc. IEEE 6th International Conference on Optimization and Applications (ICOA)*, Beni Mellal, Morocco, 2020, pp. 1-8.

[3] N. K. Nguyen, P. Wira, D. Flieller, D. O, Abdeslam, and J. Merckle, "Harmonics identification with artificial neural networks: application to active power filtering", *International Journal of Emerging Electric Power Systems*, vol. 12, no. 5, 2011.

[4] R. N. Beres, X. Wang, M. Liserre, F. Blaabjerg, and C. L. Bak, "A review of passive power filters for three-phase grid-connected voltage-source converters," *IEEE J. Emerg. Select. Top. Power Electron.*, vol. 4 , no. 1, 2016.

[5] P. Salmerón and S. P. Litrán "Improvement of the electric power quality using series active and shunt passive filters," *IEEE Trans. Power Deliv.*, vol. 25, no. 2, pp. 1058-1067, 2010.

[6] H. Suyono, R. N. Hasanah, and E. P. Widyananda, "Power system optimization of static VAR compensator using novel global harmony search method," *International Journal of Electrical and Electronic Engineering & Telecommunications*, vol. 8, no. 1, pp. 26-32, January 2019.

[7] C. Lachkar, *et al*., "Failure analysis of aluminum electrolytic capacitors based on electrical and physicochemical characterizations," presented at the 2017 IEEE International Reliability Physics Symposium (IRPS), April 2017.

[8] L. F. Costa and M. Liserre, "Failure analysis of the DC-DC converter: A comprehensive survey of faults and solutions for improving reliability," *IEEE Power Electron. Mag*., vol. 5, no. 4, pp. 42-51, 2018.

[9] W. Rohouma, R. S. Balog, A. A. Peerzada, and M. M. Begovic, "D-STATCOM for harmonic mitigation in low voltage distribution network with high penetration of nonlinear loads," *Renewable Energy*, vol. 145, pp. 1449-1464, June 2019.

[10] J. Hussain, M. Hussain, S. Raza, and M. Siddique, "Power quality improvement of grid connected wind energy system using DSTATCOM-BESS," *International Journal of Renewable Energy Research*, vol. 9, no. 3, pp. 1388-1397, September 2019.

[11] P. S. Revuelta, S. P. Litrán, and J. P. Thomas, "Hybrid filters: series active power filters and shunt passive filters," in *Active Power Line Conditioners Design, Simulation and Implementation for Improving Power Quality*, 1st Edition, Elsevier, 2016, pp. 189-229.

[12] K. R Uyyuru, M. K Mishra, and A Ghosh, "An optimization-based algorithm for shunt active filter under distorted supply voltages," *IEEE Trans Power Electr*., vol. 24, no. 5, pp. 1223-1232, 2009.

[13] S. Rahmani, A. Hamadi, K. Al-Haddad, and H. Y. Kanaan, "A multifunctional power flow controller for photovoltaic generation systems with compliance to power quality standards," in *Proc. 38th Annual Conference on IEEE Industrial Electronics Society*, 2012, pp. 894-903.

[14] R. Noroozian and G. B. Gharehpetian, "An investigation on combined operation of active power filter with photovoltaic arrays," *Electrical Power and Energy Systems*, vol. 46, pp. 392–399, Mar. 2013.

[15] Y. A. El Kadi, Y. Lakhal, and F. Z. Baghli, "Compensation of the harmonic pollution by photovoltaic systems under variable solar radiation," in *Proc. International Conference of Computer Science and Renewable Energies (ICCSRE)*, Agadir, Morocco, 2019, pp. 1-4.

[16] F. H. gandoman, A. Ahmadi, A. M. Sharaf, P. Siano, J. Pou, B. Hredzak, and V. G. Agelidis, "Review of facts technologies and applications for power quality in smart grids with renewable energy systems," *Renewable and Sustainable Energy Reviews*, vol. 82, pp. 502-514, February 2018.

[17] D. Fallows, S. Nuzzo, A. Costabeber, and M. Galea, "Harmonic reduction methods for electrical generation: A review," *IET Generation, Transmission & Distribution*, vol. 12, no. 13, pp. 3107-3113, July 2018.

[18] E. S. Sreeraj, K. Chatterjee, and S. Bandyopadhyay, "One-cycle-controlled single-stage single-phase voltage-sensorless grid-connected PV system," *IEEE Trans. on Industrial Electronics*, vol. 60, no. 3, pp. 1216-1224, 2013.

[19] N. R. Tummuru, M. K. Mishra, and S. Srinivas, "Multifunctional VSC controlled microgrid using instantaneous symmetrical components theory," *IEEE Trans. on Sustainable Energy*, vol. 5, no. 1, pp. 313-322, January 2014.

[20] Y. Aitelkadi, F. Z. Baghli, and Y. Lakhal, "Harmonic pollution compensation by connected photovoltaic systems using the instantaneous power method," *International Journal of Advanced Research*, vol. 6, no. 11, pp. 526–536, 2018.

[21] R. S. Herrera and P. Salmerón, "Instantaneous reactive power theory: A reference in the nonlinear loads compensation," *IEEE Trans Ind. Electr.*, vol. 56, no. 6, pp. 2015-2022, 2009.

[22] B. Liu and R. Jordan, "Daily insolation on surfaces tilted towards equator," *Trans. ASHRAE*, vol. 67, pp. 526-541, 1962.

[23] D. Colienne, M. Journée, and C. Bertrand, "Evaluation of different models to estimate the global solar radiation on inclined surfaces," *Renewable Energy*, vol. 50, no. 3, pp. 710-721, 2013.

[24] N. Yang, H. Liu, L. Zhao, and C. Xu, "Performance evaluation of hourly solar radiation models on inclined surfaces in Longdong Area, China," in *Proc. IOP Conf. Series: Earth and Environmental Science*, 2019.

[25] X. Wang and F. Blaabjerg, "Harmonic stability in power electronic-based power systems: Concept, modeling, and analysis," *IEEE Trans. on Smart Grid*, vol. 10, no. 3, pp. 2858-2870, May 2019.

[26] S. Rahmani, N. Mendalek, and K. Al-Haddad, "Experimental design of a nonlinear control technique for three-phase shunt active power filter", *IEEE Trans. on Industrial Electronics*, vol. 57, no. 10, pp. 3364-3375, 2010.

[27] M. Ravindra and D. G. Kumar, "Design of VSI based STATCOM for eliminating harmonic currents due to non linear load and to compensate the reactive power in a grid connected system," *International Journal of Engineering Research and Applications (IJERA)*, vol. 2, no. 6, pp. 436-443, 2012.

[28] N. Narasimhulu and K. Swathi, "Adaptive filter implementation for DSTATCOM," *International Journal of Advanced Research in Electrical, Electronics and Instrumentation Engineering*, vol. 5, no. 6, June 2016.

[29] R. M. Reddy and B. S. Reddy "Adaptive filter implementation based control algorithm for distribution static compensator," *World Wide Journal of Multidisciplinary Research and Development*, vol. 4, no. 2, pp. 345-354, 2018;

[30] M. Mahdianpoor, A. Kiyoumarsi, M. Ataei, R. A. Hooshmand, and H. Karimi, "A multifunctional DSTATCOM for power quality improvement," *Turkish Journal of Electrical Engineering & Computer Sciences*, vol. 25, pp. 172-183, 2017.

[31] K. Prabaakaran, S. Krishnakumar, R. Srividhya, R. R. Ganesh, R. Gotham, and R. Tamilarasan, "Power quality enhancement in microgrid with DSTATCOM using modified reinforcement learning algorithm," *Journal of Physics*: *Conference Series 1362, International Conference on Physics and Photonics Processes in Nano Sciences*, 2019.

[32] S. R. Arya, B. Singh, R. Niwas, A. Chandra, and K. Al-Haddad, "Power quality enhancement using DST ATCOM in distributed power generation system," *IEEE Trans. on Industry Applications*, vol. 52, no. 6, pp. 5203-5212, 2016.

[33] B. Singh, S. R. Arya, A. Chandra, and K. Al-Haddad, "Implementation of adaptive filter in distribution static compensator," *IEEE Trans. on Industry Applications*, vol. 50, no. 5, pp. 3026-3036, 2014.

[34] Z. Zeng, H. Yang, R. Zhao, and C. Chen, "Topologies and control strategies of multi-functional grid connected inverters for power quality enhancement: A comprehensive review," *Renewable and Sustainable Energy Reviews*, vol. 24, pp. 223–270, 2013

[35] A. Bouafia, J. P. Gaubert, and F. Krim, "Design and implementation of predictive current control of three-phase PWM rectifier using Space-Vector Modulation (SVM)," *Energy Conversion and Management*, vol. 51, no. 12, pp. 2473-2481, December 2010.

[36] L. Albuquerque, A. J. Moraes, G. C. Guimaraes, S. M. R. Sanhueza, and A. R. Vaz, "Photovoltaic solar system connected to the electric power grid operating as active power generator and reactive power compensator," *Solar Energy*, vol. 84, no. 7, pp. 1310–1317, July 2010.

[37] D. Rivas, L. Monin, J. W. Dixon, and J. R. Espinoza, "Improving passive filter compensation performance with active techniques," *IEEE Trans. on Industrial Electronics*, vol. 50, no. 1, pp. 161-170, 2003.

[38] M. Labben-Ben Braiek, F. Fnaiech, K. Al-Haddad, and L. Yacoubi, "Study of two current control techniques applied to a shunt active power filter," *Power Quality and Active Filtering III, Electrimacs*, pp. 1-6, Aug. 2002.

Youssef AIT EL KADI was born in 1974 in Morocco. He graduated from the aggregation in electrical engineering in 2000 in ENSET Rabat; he graduated from the University of Ibn Zohr Morocco, and defended the doctoral thesis in 2016 in Instrumentation, Measurement, Control, Characterization and Modeling with very honors. He works in the Higher School of Technology, Sultan Moulay Slimane University, Beni Mellal, Morocco in the position of Teacher Researcher. Dr. AIT EL KADI is a permanent member of the Laboratory of Engineering & Applied Technology and team leader of Modeling and Control of Electrical, Electronic and Energy Systems (MCS3E).